Application Note

Challenges in Noise Suppression for Impedance-Based Respiration Measurement Circuitry in an Integrated AFE Architecture

Rayna Feng

ABSTRACT

This document was translated from a simplified Chinese source. (ZHCAG71)

Respiration measurement is one of the common indicators in patient monitoring systems and is typically implemented by impedance pneumography, where an AC excitation signal is used to detect changes in thoracic impedance during respiration to derive the respiratory waveform. In real-world clinical monitoring scenarios, to safely and accurately extract the extremely small thoracic impedance variations during respiration, the design of the respiration measurement circuitry must address complex noise-suppression challenges. In accordance with IEC 60601 and the noise specification requirements of modern monitors, this document discusses the design challenges and solutions for respiration measurement circuitry based on AFE architectures, and provides actual test results using the AFE159RP4 as an example.

Table of Contents

List of Figures

List of Tables

1 Introduction

In patient monitoring systems, the respiration measurement system commonly uses impedance pneumography to monitor respiratory activity. Among the various methods of impedance pneumography, the constant-current method offers superior safety and imposes relatively low requirements on skin preparation, making it the most widely adopted method.

In practical hardware architecture, impedance measurement is typically realized using a two-electrode configuration. In this method, an excitation current is injected through a pair of electrodes, and based on $\Delta U = I \times \Delta R$, the same electrode pair is used to extract the voltage, thereby indirectly reflecting changes in thoracic impedance. According to the measurement principle of the two-electrode method, a high-frequency current carrier is capacitively coupled into the human body, and the low-frequency thoracic impedance variation is amplitude-modulated onto the carrier. After demodulation, the resulting impedance signal comprises a weak AC component representing respiratory activity and a DC component representing the baseline thoracic impedance.

The impedance-based respiration measurement circuitry has evolved from discrete designs to today's mainstream integrated analog front-end (AFE) architectures, such as the ADS129xR series and AFE159RPx series. The advantage of integrated AFEs lies in the high integration of complex circuits such as the excitation source, instrumentation amplifier, demodulation circuit, and high-resolution ADC, which not only reduces the circuit footprint and signal transmission paths but also significantly enhances the system's common-mode rejection ratio (CMRR). However, integration has not eliminated the challenges posed by noise. Since amplification and demodulation are performed within the chip, external input protection circuits, lead impedance matching, and PCB layout become the new bottlenecks affecting performance. If external suppression is inadequate, the chip's internal high-precision advantage will be completely masked by interference injected at the front end. Therefore, in the context of high integration, external hardware noise suppression has become the determining factor for system sensitivity and accuracy.

2 Principles of Respiration Impedance Measurement

2.1 Thoracic Impedance Measurement Model

The complete equivalent circuit of a single biological cell is shown in Figure 2-1A. Within the low-frequency range commonly used in patient monitors (below 1 MHz), the cell-membrane leakage resistance R_m is extremely large and the parallel capacitances of the intracellular and extracellular fluids C_i and C_e are extremely small; therefore, all can be considered as open circuits. This can be simplified into the parallel equivalent circuit model shown in Figure 2-1B (also known as the R-C three-element model). The macroscopic electrical properties of thoracic tissues follow the same model [1]. Because the cell-membrane capacitive reactance C_m decreases significantly in the 50kHz–100kHz range, current can penetrate the cell membrane and enter the intracellular fluid R_i. At this point, the overall impedance of the lung tissue (comprising alveoli, blood, and interstitial fluid) exhibits the highest sensitivity and best linearity in response to changes in gas volume. Considering these factors alongside safety requirements, the respiratory excitation frequency is typically set within the range of 20kHz to 100kHz.

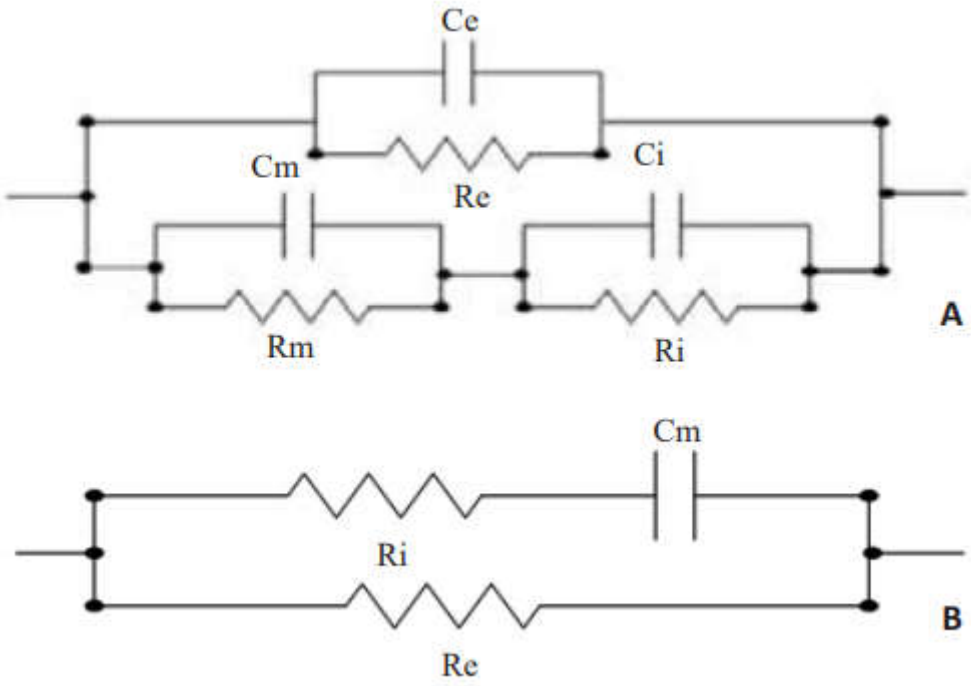

Figure 2-1. Biological Impedance Equivalent Model

Figure 2-2 illustrates the equivalent physical model of respiration measurement based on the four-electrode method, where C and D are the high-frequency constant-current excitation electrodes, and E and F are the high-impedance voltage measurement electrodes. By simulating changes in internal physical characteristics, this model reveals the fundamental essence of impedance pneumography [2]:

1. Uniform field distribution (Figure 2-2a): Under ideal uniform tissue distribution, the current field formed by the excitation current within the body is uniform. In this case, the voltage equipotential surfaces are horizontally linear, allowing the E-F sensing electrodes to pick up a stable reference potential difference.
2. Low-impedance interference effect (Figure 2-2b): When a highly conductive medium (e.g., a low-resistivity metal block) is introduced inside the tissue, the "shunt effect" causes current lines to concentrate toward the high-conductivity area, distorting the local current field. In this case, the voltage equipotential surfaces contract, reducing the potential difference between sampling points J and K.
3. High-impedance obstruction effect (Figure 2-2c): Conversely, if a non-conductive medium (e.g., an insulating plastic sphere, simulating lung inflation) is introduced, current lines are forced to bypass it, increasing local current density and making voltage equipotential surfaces denser. In this case, the potential difference between sampling points J and K increases accordingly.

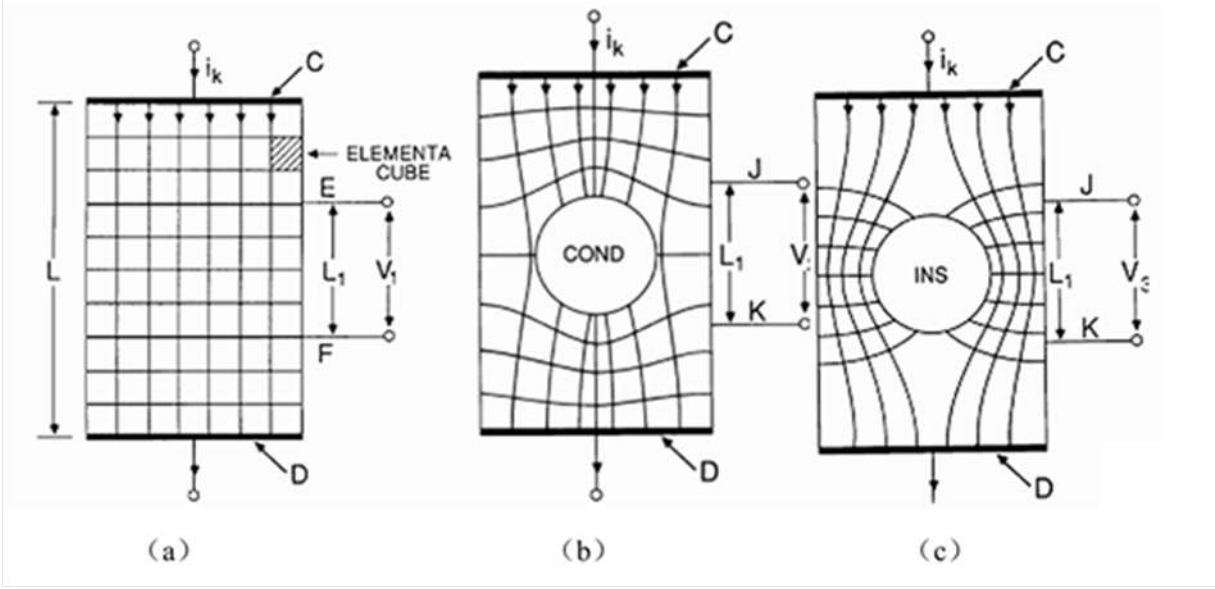

Figure 2-2. Human Respiration Model

This model demonstrates that human respiration-induced changes in lung impedance essentially alter the distribution of the internal current field, which in turn reconfigures the equipotential surfaces of the body surface voltage. By capturing these changes in surface potential differences, the respiratory signal reflecting lung volume variations can be indirectly extracted.

During respiration measurement, the thorax presents a bio-impedance to the electrodes that consists of a relatively constant baseline component and a varying component that changes only slightly. In this document, the baseline component is referred to as the baseline impedance, denoted as $R_{Baseline}$ or R_B (typically 500Ω to 2kΩ), and the varying component as the respiration impedance, denoted as ΔR (typically 0.2Ω to 5Ω). During inspiration, the change in the air-to-fluid ratio within the lungs and the extension of conduction paths leads to a decrease in local conductivity, resulting in an increase in total thoracic impedance. This change is linearly correlated with the respiratory volume, and the respiratory rate can be measured by detecting the amplitude-modulated voltage signal generated by the high-frequency carrier current.

2.2 Modulation and Demodulation of the Respiratory Waveforms

In clinical practice, the signal chain for respiration measurement does not act directly on human tissues; rather, it must pass through a complex impedance network composed of protective components and the electrode-skin physical interface. To simplify the lead design of patient monitors and enable high integration with electrocardiogram (ECG) electrodes, the same pair of electrodes and lead wires is typically used for both injection of the respiratory excitation current and pickup of the respiratory voltage signal, i.e., the two-electrode method. In standard 3-lead or 5-lead ECG monitoring, respiration measurement is typically fixed on one of the following two lead configurations:

1. Lead I (RA-LA): Electrodes placed under the left and right clavicles near the shoulders. This is the most clinically convenient placement, but the short path and high position result in a smaller ΔR (respiration impedance variation) and make it susceptible to motion artifacts from arm movements.
2. Lead II (RA-LL): Electrodes placed under the right clavicle and on the left lower abdomen or the left mid-axillary line at the 6th intercostal space. The current path diagonally crosses the entire thorax, covering the area of maximum lung expansion. This lead configuration provides the largest ΔR amplitude and a relatively stable baseline impedance R_b.

According to the basic safety and essential performance requirements for ECG monitoring devices in IEC 60601, the respiration measurement circuit must be capable of withstanding defibrillation pulses. Therefore, series anti-defibrillation resistors are typically added symmetrically on both the excitation-injection and signal-pickup sides, with common resistance values ranging from 1kΩ to 10kΩ. According to ANSI/AAMI EC13, the polarization impedance of a single electrode is typically modeled as a parallel resistor-capacitor network (51kΩ

|| 47mF) [3]. At high frequencies, the capacitor provides an effective bypass, reducing the electrode impedance from tens of kilohms at DC to a few tens of ohms. As a result, the excitation current can readily pass through the electrode interface into the body.

Figure 2-3 illustrates a simplified model of the respiration measurement circuit. In the respiration measurement circuit, the baseline impedance of the human body R_B, the anti-defibrillation resistors Rp, and the electrode polarization impedance Z_E together constitute the total baseline impedance of the respiration measurement. The total circuit impedance $Z_{total}(t)$ is given by:

$$Z_{total}(t) = 2R_p + R_B + 2|Z_E| + \Delta R(t) = R_{static} + \Delta R(t) \quad (1)$$

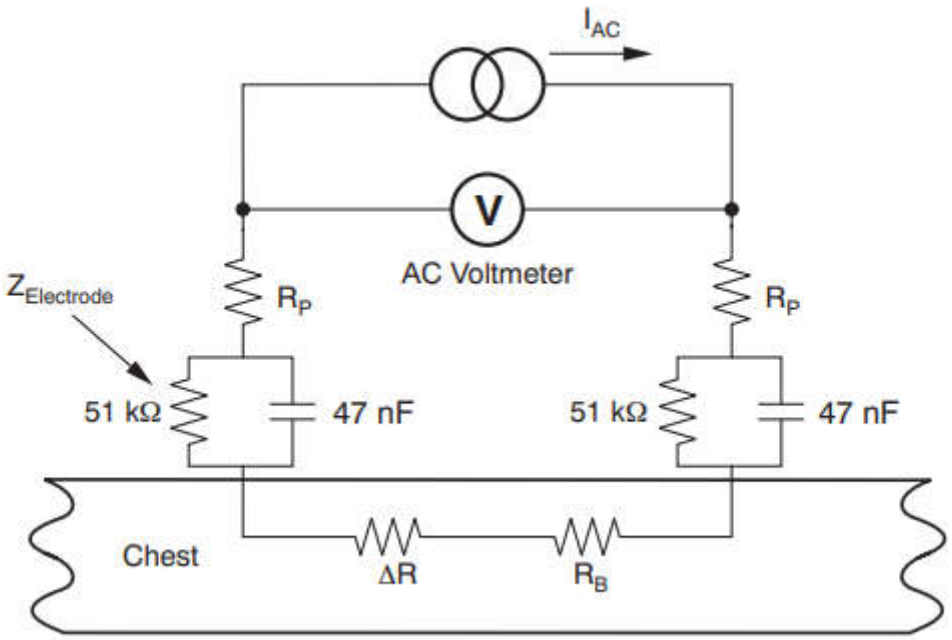

Figure 2-3. Respiration Measurement Circuitry Model

The excitation signal I_{AC} is typically a constant-current drive with a frequency between 20kHz and 100kHz and an RMS value below 500μA. In this frequency range, the contact impedance between the skin and electrodes is significantly reduced, and the current does not stimulate nerves or cardiac muscle, avoiding the risk of micro-shock.

Assuming the excitation current is a sine wave I_{sine} (t) = I_{mcos} (ωt), the differential voltage picked up is:

$$V(t) = I_{sine}(t) \cdot Z_{total}(t) = I_m[R_{static} + \Delta R(t)]\cos(\omega t + \varphi) \quad (2)$$

where φ is the total system phase shift caused by the complex impedance of the body, lead-wire distributed capacitance, and polarization capacitance.

Multiplying V(t) by the in-phase reference signal Acos(ωt) and passing through a low-pass filter to remove the doubled-frequency term cos(2ωt + φ) yields:

$$V_{demod} = \frac{1}{2}AI_m[R_{static} + \Delta R(t)]\cos(\varphi) \quad (3)$$

The AC component $\frac{1}{2}AI_m\cos(\varphi) \cdot \Delta R(t)$ is the desired respiratory signal. It can be observed that coherent demodulation is very sensitive to phase variations. In practice, quadrature demodulation can eliminate the influence of cos(φ) and enhance system robustness.

Assuming the excitation current is a square wave, multiple harmonic components must be considered. According to the Fourier series expansion, it can be expressed as $I_{sq}(t) = \frac{4I}{\pi}\sum_{n=1,3,5...}^{\infty}\frac{1}{n}\sin(n\omega t)$. The picked-up differential voltage includes both the static carrier term and the modulation term containing respiration information:

$$V(t) = I_{sq}(t) \cdot Z_{total}(t) = [R_{static} + \Delta R(t)]\frac{4I}{\pi}\sum_{n=1,3,5...}^{\infty}\frac{1}{n}\sin(n\omega t + \varphi) \quad (4)$$

Multiplying V(t) by the in-phase reference signal $\frac{4}{\pi}\sum_{k=1,3,5...}^{\infty}\frac{1}{k}\sin(n\omega t)$ and then passing through a low-pass filter to remove all terms containing ω and its multiples, it can be obtained using the Bessel series properties:

$$V_{demod} = I[R_{static} + \Delta R(t)]\cos(\varphi) \quad (5)$$

where φ is the total system phase shift caused by the complex impedance of the body, lead-wire distributed capacitance, and polarization capacitance.

The AC component Icos(φ) * ΔR(t) is the desired respiratory signal. In the ideal case, square-wave demodulation incurs no gain conversion loss. However, in engineering practice, since φ cannot be exactly zero and square-wave edge jitter exists, demodulation gain loss and nonlinear distortion may occur. To address this, the ADS1296R introduces a Blocking signal that creates a sampling blind zone at signal transition edges, minimizing the transient interference and ensuring stable post-demodulation amplitude gain.

3 Noise Suppression in Respiration Measurement Circuitry

In medical monitoring scenarios, respiration waveforms are primarily used to assess a patient's breathing status in real time to detect respiratory issues in a timely manner. A normal respiratory waveform exhibits a regularly undulating, quasi-sinusoidal shape, including an inspiratory phase (rising edge) and an expiratory phase (falling edge). Accurate respiratory waveforms help promptly identify acute conditions such as respiratory failure and airway obstruction, evaluate spontaneous breathing ability in patients recovering from anesthesia, and observe improvements in respiratory function. The challenge in designing impedance-based respiration measurement systems lies in extracting a respiration impedance signal that does not exceed 1 ohm from a background impedance in the range of several thousand ohms. Therefore, the system's noise suppression level directly determines the accuracy and reliability of the respiratory waveform and has significant clinical value.

3.1 Respiratory Noise Test Method and Specification Requirements

In engineering practice, relative noise is typically used to evaluate the noise of a respiration measurement system. With a fixed baseline impedance, the system's peak-to-peak noise N_{pp} at ΔR = 0Ω and the peak-to-peak respiratory signal S_{pp} at ΔR = 1Ω are measured separately, with a recommended duration of more than 10 seconds. The ratio of these two peak-to-peak values $N_{pp}|S_{pp}$ represents the respiratory noise of the system, measured in ohms (Ω). This ratio physically represents the proportion of noise per unit impedance signal. This measurement method essentially uses the concept of signal-to-noise ratio and provides a simple, efficient way to measure the system's relative noise level, making it very practical in engineering.

If this ratio exceeds 10%, i.e., the respiration measurement system's noise exceeds 100mΩ, the system has a high risk of missing weak respiratory signals. Currently, high-precision patient monitors in the medical device industry typically require this ratio to be below 10% (i.e., the respiratory noise below 100mΩ) to ensure stable and accurate respiratory waveform extraction in complex clinical environments.

3.2 Challenges in Design of Respiration Measurement Circuitry

Based on the aforementioned principle of impedance-based respiration measurement, from a discrete design perspective, the respiration measurement circuitry primarily consists of two parts: carrier generation and signal acquisition. The carrier generation circuit provides both the excitation (modulation) signal and the demodulation reference signal. Its structure depends on the waveform type; for example, square waves can be generated using a 555 timer or multi-vibrator, while sine waves can be generated using the DDS (Direct Digital Synthesis) method. The signal-acquisition circuit samples the respiration impedance and the circuitry mainly includes capacitive coupling, amplification/filtering, modulation/demodulation, and ADC conversion circuits.

TI's medical monitoring AFE products highly integrate most of the above circuits. Figure 3-1 illustrates the respiration measurement circuit module integrated within the ADS1296R: the respiration clock generator divides the master clock to generate the excitation, demodulation, and blocking signals. By configuring the respiration-related control registers, the chip outputs a square-wave excitation signal at 32kHz or 64kHz through pins RESP_MODP and RESP_MODN. The amplitude-modulated respiratory signal goes from pins IN1P and IN1N to the signal processing circuit within the chip through the lead wires and external hardware, and passes through internal filtering, amplification, and demodulation modules before entering the ADC for analog-to-digital conversion.

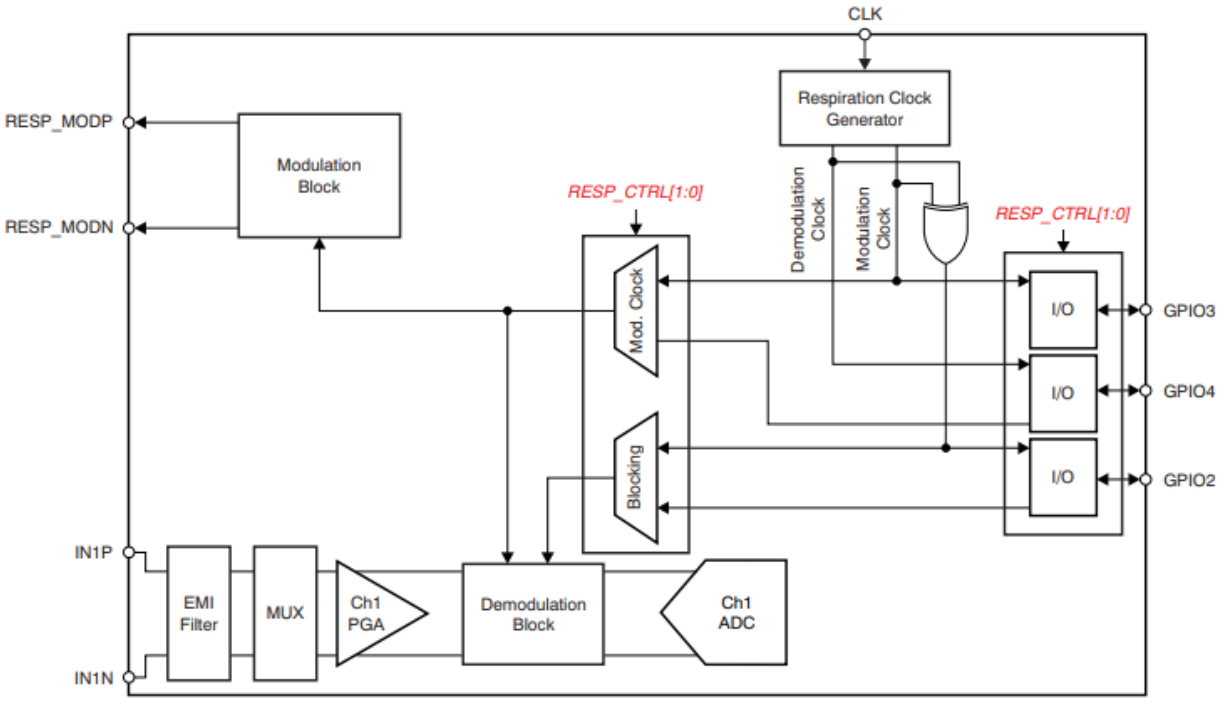

Figure 3-1. Respiration Measurement Circuitry Within ADS1296R

Based on an integrated AFE architecture, the external respiration measurement circuitry determines the upper limit of the overall signal-to-noise ratio of the system, and its design faces the following challenges:

1. For an integrated AFE, the internal dynamic range is fixed. If the external measurement circuitry is not properly designed, high-frequency noise will be directly introduced into the AFE's sampling front end, causing aliasing that raises the noise floor and may even drown the weak respiration impedance signal in quantization noise.
2. Currently available mainstream AFE chips can achieve a common-mode rejection ratio (CMRR) as high as 140dB; therefore, the parameter matching between the external AC coupling capacitors and the biasing network directly impacts the common-mode rejection capability of the signal chain. Improper design will convert external interference directly into differential-mode noise in the respiratory signal.
3. For respiration impedance demodulation, if the external measurement circuitry compromises the phase consistency between the excitation signal and the demodulation clock, it will directly reduce the post-demodulation output amplitude, degrading the respiration measurement sensitivity.
4. In clinical environments, the AFE faces various challenges, such as electromagnetic interference from electrosurgical units and high-voltage pulses from defibrillators. The design of external measurement circuitry must ensure that the AFE chip operates normally under strong interference and guarantees long-term device reliability.

Therefore, when designing a respiration measurement circuitry based on the AFE architecture, adequate noise suppression is essential. Effective noise-suppression design helps users maximize the performance of the AFE chip.

3.3 Differential Balanced Design of Respiration Measurement Circuitry

According to the design requirements of multi-parameter monitors, the respiration measurement front-end conditioning circuit must support multi-lead switching and channel multiplexing, ensure safety compliance and waveform optimization of the excitation signal, and provide signal conditioning. Figure 3-2 illustrates the respiration measurement circuitry design based on an AFE architecture, which meets the clinical requirement for switching between Lead I and Lead II.

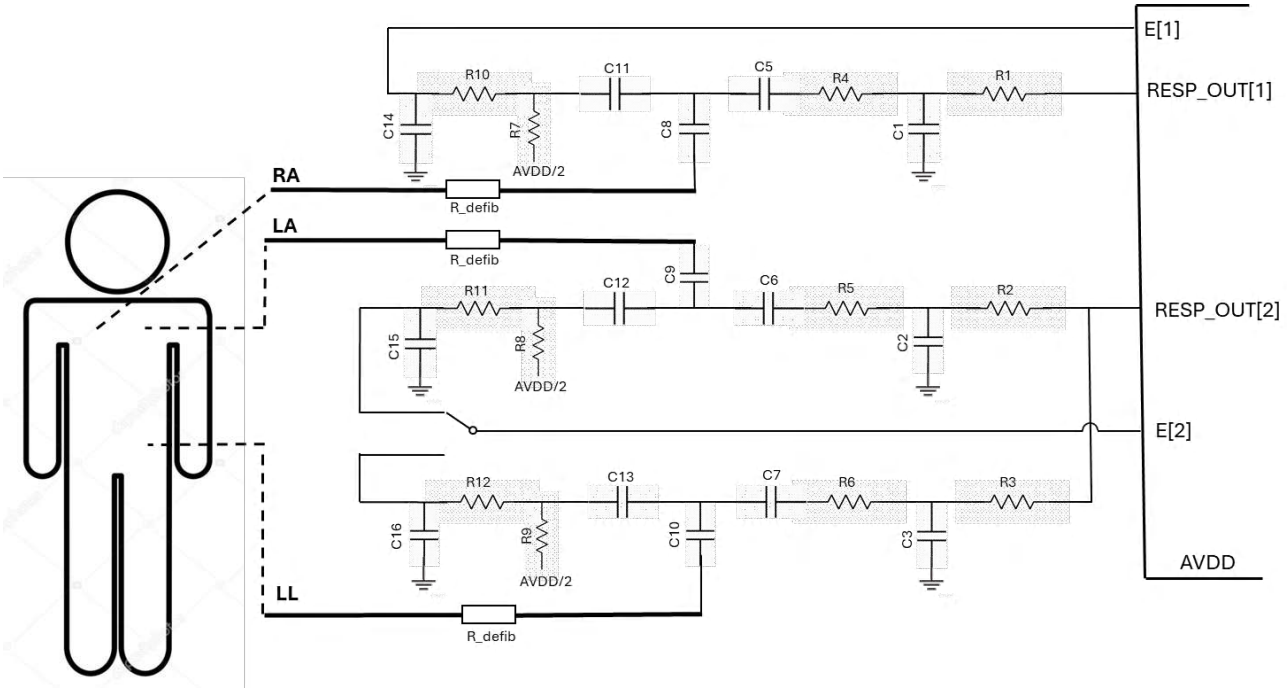

Figure 3-2. Respiration Measurement Circuitry Based on AFE Architecture

In the excitation path design, series resistors (R1–R6) are configured with values typically much larger than the human body and electrode contact impedances, converting the AFE's voltage-source characteristic into an approximate high-impedance constant-current source output. This makes the source impedance much larger than the baseline body impedance, effectively reducing excitation current fluctuations caused by changes in electrode-skin contact impedance, thereby physically eliminating measurement nonlinearity due to contact resistance variations. In addition, high-voltage capacitors (C5–C7) block any DC current from entering the body, preventing electrical burns and potential cardiac shock hazards. Their capacitive reactance must be much smaller than the series resistors (R1–R6) to avoid attenuation of the excitation signal.

For the respiration measurement system, in addition to the target respiratory signal at the carrier frequency between 20kHz and 100kHz, there are strong interfering signals such as human electrocardiographic disturbances (0.5Hz–150Hz) and 50Hz power-line noise. For the respiration measurement circuitry, a segmented conditioning approach can be adopted. For the excitation signal generated internally by the AFE, an RC low-pass filter with a cutoff frequency at 1.2 to 1.5 times the carrier frequency is formed by resistors (R1–R6) and capacitors (C1–C3). This filters out high-order harmonics of the carrier while reducing the excitation signal bandwidth, which helps minimize electromagnetic radiation from the system and ensures that the excitation current waveform exhibits a clean sinusoidal characteristic, thereby improving the impedance measurement linearity. Additionally, on the acquisition side, a high-pass filter with a cutoff frequency between 10kHz and 20kHz is formed by capacitors (C11–C13) and resistors (R7–R9). This provides deep attenuation of over 40dB against ECG baseline drift and the P-Q-R-S-T wave complex, preventing electrocardiographic disturbances from affecting the respiration measurement. Before the AFE inputs, an anti-aliasing filter with a cutoff frequency below half the ADC sampling rate formed by resistors (R10–R12) and capacitors (C14–C16) also ensures the system robustness against ultra-high-frequency noise from external electrosurgical units and similar sources.

To cancel power-line noise in strong-interference environments such as operating rooms, the RC filter components must be made of high-precision and high-stability materials. It is recommended to use thin-film

resistors with a precision of 0.1% and C0G capacitors with a precision of 1%. Furthermore, strict symmetrical routing guidelines must be followed to ensure that common-mode noise maintains high phase consistency before entering the AFE, thereby leveraging the AFE's high CMRR to substantially cancel it out.

For example, with the above measurement circuitry used, AFE159RP4 can provide the respiration noise test results as shown in Table 3-1, and its performance significantly exceeds the test requirement of <10%.

Table 3-1. Respiration Noise Test Results with AFE159RP4

Sampling rate (Hz)	Respiration rate (rpm)	Respiration amplitude (mV)		Noise (Ω)
		S_{pp}	N_{pp}	N_{pp}/S_{pp}
2k	20	0.329	0.015	0.045
	40	0.336	0.016	0.046
	60	0.339	0.017	0.049

4 References

1. Yang Jianming. *A Method for Measuring Pulmonary Function Parameters Based on Thoracic Impedance*
2. Baker, L.E. *Applications of the impedance technique to the respiratory system*. IEEE Engineering in Medicine and Biology Magazine, 1989
3. SBAA181 – February 2011

IMPORTANT NOTICE AND DISCLAIMER

TI PROVIDES TECHNICAL AND RELIABILITY DATA (INCLUDING DATASHEETS), DESIGN RESOURCES (INCLUDING REFERENCE DESIGNS), APPLICATION OR OTHER DESIGN ADVICE, WEB TOOLS, SAFETY INFORMATION, AND OTHER RESOURCES “AS IS” AND WITH ALL FAULTS, AND DISCLAIMS ALL WARRANTIES, EXPRESS AND IMPLIED, INCLUDING WITHOUT LIMITATION ANY IMPLIED WARRANTIES OF MERCHANTABILITY, FITNESS FOR A PARTICULAR PURPOSE OR NON-INFRINGEMENT OF THIRD PARTY INTELLECTUAL PROPERTY RIGHTS.

These resources are intended for skilled developers designing with TI products. You are solely responsible for (1) selecting the appropriate TI products for your application, (2) designing, validating and testing your application, and (3) ensuring your application meets applicable standards, and any other safety, security, regulatory or other requirements.

These resources are subject to change without notice. TI grants you permission to use these resources only for development of an application that uses the TI products described in the resource. Other reproduction and display of these resources is prohibited. No license is granted to any other TI intellectual property right or to any third party intellectual property right. TI disclaims responsibility for, and you fully indemnify TI and its representatives against any claims, damages, costs, losses, and liabilities arising out of your use of these resources.

TI’s products are provided subject to TI’s Terms of Sale, TI’s General Quality Guidelines, or other applicable terms available either on ti.com or provided in conjunction with such TI products. TI’s provision of these resources does not expand or otherwise alter TI’s applicable warranties or warranty disclaimers for TI products. Unless TI explicitly designates a product as custom or customer-specified, TI products are standard, catalog, general purpose devices.

TI objects to and rejects any additional or different terms you may propose.

Last updated 10/2025